

NOV 17 1952

c. 1  
RM 52125

NACA RM 52125



# RESEARCH MEMORANDUM

TORSION, COMPRESSION, AND BENDING TESTS OF TUBULAR  
SECTIONS MACHINED FROM 75S-T6 ROLLED ROUND ROD

By R. L. Moore and J. W. Clark

Aluminum Company of America

NATIONAL ADVISORY COMMITTEE  
FOR AERONAUTICS

WASHINGTON

November 12, 1952

NACA LIBRARY  
LANGLEY AERONAUTICAL LABORATORY  
Langley Field, Va.



3 1176 01434 3835

1R

NACA RM 52I25

NATIONAL ADVISORY COMMITTEE FOR AERONAUTICS

RESEARCH MEMORANDUM

TORSION, COMPRESSION, AND BENDING TESTS OF TUBULAR  
SECTIONS MACHINED FROM 75S-T6 ROLLED ROUND ROD

By R. L. Moore and J. W. Clark

SUMMARY

Tests were made of tubular sections machined from 75S-T6 aluminum-alloy rolled rod and having ratios of tube diameter to wall thickness  $D/t$  ranging from 2 to 150. The purpose of the investigation was to establish curves of strength in torsion, compression, and bending against  $D/t$  for the tubular sections and to show to what extent these strengths may be correlated with the mechanical properties of the material. In view of the acceptable mechanical properties obtained for the material, the relations obtained between these strengths and  $D/t$  may be used as a tentative basis for design of members of the type investigated.

INTRODUCTION

The tests described in this report were undertaken in response to requests from aircraft manufacturers for information to be used in the design of tubular members of aluminum alloy 75S-T6. Although such design generally involves considerations other than simple tension, compression, and bending, as discussed herein, relations between strengths under these loadings and ratios of tube diameter to wall thickness  $D/t$  constitute essential design data. These tests were made on round sections machined from 75S-T6 rolled round rod, and having  $D/t$  ratios ranging from 2 to 150; they supplement some earlier tests of the same kind made on 75S-T6 extruded tubing.

It was the object of this investigation to establish curves of strength in torsion, compression, and bending against ratios of diameter to wall thickness  $D/t$  for the tubular sections and to show to what extent these strengths may be correlated with the mechanical properties of the material.

This work was done by the Aluminum Company of America and has been made available to the National Advisory Committee for Aeronautics for publication because of its general interest.

#### MATERIAL

Test specimens were cut from five 12-foot lengths of 2-inch-diameter 75S-T6 rolled round rod. Average mechanical properties for this lot of material are listed in table I. The longitudinal tensile properties are above guaranteed minimum values for 75S-T6 rods, bars, and shapes (reference 1), and above the values recommended for design in reference 2. Figure 1 shows longitudinal and transverse stress-strain curves in tension and compression for specimens cut from one of the rods. The tensile strength and tensile and compressive yield strengths for these specimens were all within 1.6 percent of the average values listed in table I. The stress-strain curves from which an average yield strength in shear was selected are shown in figure 10.

#### SPECIMENS AND TEST PROCEDURE

The tests were made on specimens of the type shown in the photographs in figures 2 to 6 and in the sketches in figures 7 to 9. Dimensions of the test sections are given in tables II, III, and IV. The tubular specimens were made by first turning down the reduced section to approximate size in a lathe, boring and reaming the hole, and finally finishing the exterior of the reduced section and cutting to length. Measurements made on cut specimens after completion of the tests indicated that maximum and minimum thicknesses were within  $\pm 0.002$  inch of the average values listed in tables II, III, and IV. In terms of percent of the average thickness, the maximum variation from the average was 6.5 percent for the tension specimens, 3.0 percent for the compression specimens, and 4.5 percent for the beam specimens.

The torsion tests were made in an Amsler Torsion Machine of 1200 foot-pound capacity. Intermediate torque ranges of 240, 400, and 800 foot-pounds were used in addition to the maximum range. Measurements of shear strain were obtained for the three specimens with the smallest D/t ratios (2, 10, and 15) by means of Amsler troptometers, graduated in degrees, fastened to the specimens near the ends of the reduced test sections. Snug-fitting steel plugs, having a length of about 4 inches, were inserted in the ends of the tubular specimens before gripping in the testing machine.

The compression specimens were tested in a Southwark-Emery 50,000-pound capacity testing machine and an Amsler 300,000-pound capacity testing machine, using appropriate load ranges. As is shown in figures 4 and 8, the specimens originally had a 6-inch-long reduced section with a short length of thicker material at each end. This design was adopted since it provided the same type of transition at the ends of the reduced test sections in all three types of specimens. Since all of the compression specimens failed at the end of the reduced portion, it was questioned whether the strength was influenced by the geometry of the shoulder. Following the first tests, therefore, the ends and the buckled portion of the test sections were cut off and the remaining length of undamaged uniform section subjected to retest.

The bending tests were made in an Amsler 40,000-pound capacity machine, using the loading fixtures shown in figure 2. These fixtures were designed and fabricated at the Aluminum Research Laboratories in 1937 and have been used in previous investigations of this kind (reference 3). Since the bending specimens could not be made more than about 22 inches long with the boring and reaming tools readily available, the effective length for test purposes was increased by the use of steel-plug extensions having a drive fit in each end. The specimens were supported at the ends and at the intermediate load points by snug-fitting yokes with knife-edge supports in the plane of the neutral axis. The end yokes were mounted on rollers in order to minimize restraint against horizontal movement of the ends accompanying vertical deflections. Deflection measurements were made on six of the beams with small  $D/t$  ratios by means of a dial gage, graduated to 0.001 inch, with suitable extensions. The deflection of the tube relative to the beam of the testing machine was measured at the center and near each end of the reduced section of the tube. In the test of the solid round specimen the dial gage readings were supplemented by measurements with a steel scale graduated to 1/50 inch. The scale was also used to determine the deflection of this specimen at the load points. Although these latter measurements were not made in the other tests, the deflection of the load points was indicated by the autographic diagrams from the testing machine.

## RESULTS AND DISCUSSION

### Torsion Tests

Table II gives the maximum torques and the corresponding average shear stresses at failure for the torsion specimens. For all except the solid specimen ( $D/t = 2$ ), the shear stresses were computed by the following formula, based on the assumption of a uniform shear stress over the thickness of the tube wall:

$$F_{st} = \frac{12T}{2\pi r^2 t} \quad (1)$$

where

$F_{st}$	average shear stress at failure, psi
$T$	torque producing failure, ft-lb
$r$	mean radius, in.
$t$	wall thickness, in.

For the solid specimen the value of the uniform shear stress assumed at failure was computed by the formula

$$F_{st} = \frac{144T}{\pi D^3} \quad (2)$$

where  $D$  is diameter of the rod in inches.

The difference shown in table II between the shear stresses computed for the solid specimen 10, and the tubular specimens 8, 9, and 11, which also fractured without buckling, apparently reflects the inaccuracy of the assumption of a uniform distribution of the shear stress in specimen 10. A closer approach to such a condition would be expected in a material having more ductility than 7S-T6. The average stress of 53,900 psi determined from the values given for specimens 8, 9, and 11 is believed to represent a more reliable value of torsional shear strength for the material.

Photographs of the torsion specimens after failure are shown in figure 3. With the exception of the four specimens noted above, all failed by buckling. Secondary fractures were obtained in many cases after buckling, however, as shown in figure 3(a).

Figure 7 shows the result obtained by plotting average shear stresses at failure against ratios of  $D/t$ . The test points in the range of  $D/t$  ratios greater than about 50 agree closely with the theoretical solution of Batdorf, Stein, and Schildcrout for elastic buckling of thin-walled cylinders with simply supported edges (reference 4). The curve obtained from this solution is also shown in figure 7. Using 0.33

as the value of Poisson's ratio  $\mu$ , the above solution can be represented for tubes of the proportions used in this investigation by the approximate formula:<sup>1</sup>

$$F_{st} = 0.75 \left(\frac{t}{r}\right)^{5/4} \left(\frac{r}{L}\right)^{1/2} E \quad (3)$$

where

E modulus of elasticity, psi

r mean radius, in.

L length of test section, in.

Since the values of  $L/r$  listed in table II were nearly constant for the various tubular specimens, an average value was substituted in equation (3) to obtain the corresponding curve in figure 7.

If the modulus of elasticity  $E$  is expressed in terms of the modulus of elasticity in shear  $G$ , equation (3) may be written

$$F_{st} = 2.0G \left(\frac{t}{r}\right)^{5/4} \left(\frac{r}{L}\right)^{1/2} \quad (4)$$

In figure 7, equation (4) has been extended into the plastic stress range by substituting the shear secant modulus  $G_s$  for  $G$ . This procedure has previously been suggested as an approximate method of predicting the critical shear stresses for flat plates (references 5 and 6). Values of  $G_s$  were determined from the shear stress-strain curve shown in figure 10(a). The shear secant-modulus curve in figure 7 gives close agreement with test values except for the specimens with  $D/t$  ratios of 10 and 15, where the theoretical curve is conservative by about 10 percent.

Also shown in figure 7 is an empirical shear-buckling curve based on tests of tubes of the lower strength aluminum alloys (reference 7). Except for the range of low  $D/t$  ratios the test values are lower than this curve, the maximum discrepancy being about 12 percent.

---

<sup>1</sup>This formula is applicable when  $100 < \frac{L^2}{rt} \sqrt{1 - \mu^2} < 10 \left(\frac{r}{t}\right)^2$ .

The torsional strengths observed in these tests ranged from about 5 to 25 percent higher than those obtained in previous tests of specimens machined from 75S-T6 extruded tubing. The spread between the two sets of test values increased with increasing ratios of D/t. A considerable part of these differences may be attributed, it is believed, to the greater uniformity in wall thickness and diameter attained in the specimens made from the rod. The latter were machined on both inside and outside, whereas the tubing specimens were machined on the outside only.

In figure 10 are plotted shear stress-strain curves for the torsion specimens with D/t ratios of 10 and 15. Shear stress was computed by equation (1), and shear strain at the mean fiber was obtained by the formula:

$$\alpha = \frac{\pi}{180} \frac{r\phi}{L} \quad (5)$$

where

- $\alpha$  shear strain at mean fiber, in./in.
- $r$  mean radius, in.
- $\phi$  total twist, deg
- $L$  gage length over which total twist is measured, in.

Figure 11 shows a similar curve for the solid round specimen plotted in terms of extreme fiber stress, assuming elastic action, against shear strain at the extreme fiber. These stresses were computed by the equation:

$$s = \frac{Tr}{J} \quad (6)$$

where

- $s$  shear stress at extreme fiber, psi
- $T$  torque, in-lb
- $r$  radius, in.
- $J$  polar moment of inertia, in.<sup>4</sup>

The slopes of the straight-line portions of the curves in figures 10 and 11 correspond to a modulus of elasticity in shear of 3,900,000 psi.

### Compression Tests

The ultimate stresses reached in the compressive tests of tubular specimens are listed in table III and plotted in figure 8. Photographs of the specimens after failure are shown in figures 4 and 5. In both sets of tests, with and without the thick-end section, the specimens failed near the end of the test section, forming from one to six buckles around the circumferences, depending on the thickness. The compressive strengths found in the second series of tests, with the specimens machined down to a  $4\frac{1}{2}$ -inch-long uniform section, were 1.5 to 7.3 per cent higher than the strengths of the same specimens in the first tests.

In the elastic-stress range, the theoretical buckling strength for a thin-walled cylinder of intermediate length and no initial defects is (reference 8):

$$F_{cc} = \frac{Et}{r\sqrt{3(1 - \mu^2)}} \quad (7)$$

where

$F_{cc}$  compressive strength, psi

$r$  mean radius, in.

$\mu$  Poisson's ratio

Critical compressive stresses for actual cylinders have been found to fall below the values given by equation (7) by an amount depending upon the size and nature of initial imperfections in the material and the geometry of the cylinders (reference 9). Though numerous empirical expressions for critical stress have been suggested on the basis of test results, they have generally been applied to cylinders with  $D/t$  ratios considerably greater than the values for the tubes used in these tests.

If the expression for critical stress of the tubes of this investigation is assumed to take the form of equation (7), and the coefficient of  $Et/r$  is based on the average strength of the two specimens having a  $D/t$  ratio of about 150, which failed in the elastic-stress range of the material, the resulting equation is:

$$F_{cc} = 0.42 \frac{Et}{r} \quad (8)$$

This equation is plotted with the test results in figure 8. The coefficient of 0.42 given above is 31 percent lower than the theoretical value for perfect shells according to equation (7). It is also slightly lower than the coefficient of 0.45 used as a basis for determining the compressive strength of seamless tubes in reference 10.

It is pointed out in reference 11 that an equation of the form of equation (8) may be used to predict buckling of curved magnesium-alloy sheet panels in the plastic stress range if the secant modulus  $E_s$  is substituted for  $E$ . The result of this substitution in equation (8), using the secant modulus determined from the longitudinal compressive stress-strain curve in figure 1(b), is shown in figure 8. Also shown in figure 8 is the curve obtained by substituting the tangent modulus  $E_t$  for  $E$  in equation (8). In general, the test points lie closer to the tangent-modulus curve.

#### Bending Tests

Table IV gives the maximum loads for the beam specimens and the corresponding moduli of failure in bending computed by the formula:

$$F_b = \frac{Mc}{I} \quad (9)$$

where

- $F_b$       modulus of failure in bending, psi
- $M$         bending moment at maximum load, in-lb
- $c$         distance from neutral axis to extreme fiber, in.
- $I$         moment of inertia of cross section, in.<sup>4</sup>

In computing the maximum bending moment at failure for the specimens having  $D/t$  ratios less than 40 it was found necessary to take into account the shortening of the moment arm of the load due to large deflections.

All specimens except the solid round specimen and the two tubes having  $D/t$  ratios of 10 failed by collapse of the tube wall and the

loads given were clearly maximum values. The loads given for the specimens which did not buckle are no doubt near the practical maximum although the tests were stopped when the knife edges reached the end of the free travel. The nature of the failures may be seen in the photographs of the specimens after testing (fig. 6).

The moduli of failure in bending are plotted against  $D/t$  ratios in figure 9. Also shown in figure 9 are the corresponding estimated values of actual maximum stress at failure. The moduli of failure, of course, represent fictitious stresses when they exceed the proportional limit of the material. Values of actual maximum stress were estimated by calculating the maximum strain from the measured deflections and finding the stress corresponding to this strain on an average stress-strain curve for tension and compression. The purpose of plotting the values of estimated actual maximum stress in bending in figure 9 was to show a comparison with the compressive-strength curve from figure 8, based on tests under axial compression. The comparison indicates that for  $D/t$  ratios less than about 60 approximately the same maximum stresses were reached under the two types of loading. For a  $D/t$  ratio of about 80 the maximum stress indicated in the bending test was about 6 percent less than that developed in compression. Some previous experiments on cylinders with  $D/t$  ratios larger than those for the tubes of this investigation have indicated critical stresses in bending appreciably greater than for axial compression (references 12 and 13).

A comparison of the moduli of failure observed in these tests with those obtained for specimens machined from 75S-T6 extruded tubing shows good agreement in the range of low  $D/t$  ratios (from about 10 to 30) but higher values for the present tests in the range of higher  $D/t$  ratios. The maximum differences were about 25 percent. As indicated previously in connection with the torsion tests, the greater uniformity in dimensions attainable in specimens machined from the solid was probably largely responsible for the differences in strength noted.

Curves of nominal maximum bending stress  $M_c/I$  against deflection are plotted in figure 12 for six of the specimens having small  $D/t$  ratios. For tubes of these proportions the maximum practical load will probably be limited by deflection rather than buckling. The deflections measured in the elastic-stress range show reasonable agreement with calculated values based on a modulus of elasticity of 10,400,000 psi.

## CONCLUSIONS

The following conclusions seem justified on the basis of these tests of 75S-T6 tubular sections machined from 2-inch-diameter rolled round rod:

1. In view of the acceptable mechanical properties obtained for the material used, the relations obtained between strengths in torsion, compression, and bending and ratios of diameter to wall thickness  $D/t$  may be used as a tentative basis for design of members of the type investigated.

2. The torsional strengths of the tubes having  $D/t$  ratios greater than about 50 agreed well with the theoretical values computed for elastic buckling of tubes with simply supported edges.

3. The torsional strengths of tubes having  $D/t$  ratios from about 20 to 50 agreed well with values calculated by substituting the shear secant modulus in the equation for elastic buckling of tubes with simply supported edges. The test values for lower ratios of  $D/t$  were in closer agreement with the buckling strengths predicted by an empirical relationship based on tests of other aluminum alloys.

4. The compressive strengths  $F_{cc}$  for a  $D/t$  ratio of about 150 were within the elastic-stress range of the material and could be expressed approximately by the equation  $F_{cc} = 0.42Et/r$ , where  $E$  is modulus of elasticity and  $r$  is mean radius. The compressive strengths of the specimens having smaller  $D/t$  ratios were observed to be in fair agreement with the curve obtained by substituting the tangent modulus for the modulus of elasticity in the equation.

5. Although the moduli of failure in bending exceeded the strengths in axial compression for specimens with  $D/t$  ratios less than about 60, the estimated actual maximum bending stresses at failure were about equal to the compressive strengths of specimens with the same  $D/t$  ratios. The modulus of failure for the bending specimen with the largest  $D/t$  ratio was slightly lower than the corresponding compressive-strength value.

Aluminum Research Laboratories  
Aluminum Company of America  
New Kensington, Pa., August 1, 1949

## REFERENCES

1. Anon.: Alcoa Aluminum and Its Alloys. Aluminum Co. of Am., 1947.
2. Anon.: Strength of Metal Aircraft Elements. ANC-5a, U. S. Govt. Printing Office, May 1949, table 3.111(g).
3. Moore, R. L., and Holt, Marshall: Beam and Torsion Tests of Aluminum-Alloy 61S-T Tubing. NACA TN 867, 1942.
4. Batdorf, S. B., Stein, Manuel, and Schildcrout, Murry: Critical Stress of Thin-Walled Cylinders in Torsion. NACA TN 1344, 1947.
5. Gerard, George: Critical Shear Stress of Plates above the Proportional Limit. Jour. Appl. Mech., vol. 15, no. 1, March 1948, pp. 7-12.
6. Stowell, Elbridge Z.: Critical Shear Stress of an Infinitely Long Plate in the Plastic Region. NACA TN 1681, 1948.
7. Moore, R. L.: Torsional Strength of Aluminum-Alloy Round Tubing. NACA TN 879, 1943.
8. Timoshenko, S.: Theory of Elastic Stability. First ed., McGraw-Hill Book Co., Inc., 1936, p. 440.
9. Batdorf, S. B., Schildcrout, Murry, and Stein, Manuel: Critical Stress of Thin-Walled Cylinders in Axial Compression. NACA Rep. 887, 1947. (Supersedes NACA TN 1343.)
10. Anon.: Alcoa Structural Handbook. Aluminum Co. of Am., 1948, p. 47.
11. Schuette, E. H.: Buckling of Curved Sheet in Compression and Its Relation to the Secant Modulus. Jour. Aero. Sci., vol. 15, no. 1, Jan. 1948, pp. 18-22.
12. Lundquist, Eugene E.: Strength Tests of Thin-Walled Duralumin Cylinders in Pure Bending. NACA TN 479, 1933.
13. Donnell, L. H.: A New Theory for the Buckling of Thin Cylinders under Axial Compression and Bending. Trans. A.S.M.E., vol. 56, no. 11, Nov. 1934, pp. 795-806.
14. Anon.: Standard Methods of Tension Testing of Metallic Materials. Designation: E8-46. A.S.T.M. Standards, 1946, pt. 1B.

TABLE I.- MECHANICAL PROPERTIES OF 2-INCH-DIAMETER 75S-T6 ROLLED ROUND ROD USED

## IN INVESTIGATION OF STRENGTH OF MACHINED TUBULAR SECTIONS

[Tensile and compressive properties are averages for determinations made on three different 12-ft lengths of rod. Shear strengths are averages for two determinations. All individual strength determinations were within 4 percent of averages shown.]

Direction	0.2-percent offset yield strength (psi)			Tensile strength (psi)	Shear strength (psi) (a)		Elongation (percent in 4D)
	Tension	Compression	Shear		Double shear	Torsion	
Longitudinal	b76,100	c82,000	d38,000	b85,700	50,000	53,900	11.3
Transverse	e70,000	f76,700		c82,300	49,600		8.7

<sup>a</sup>Shear strengths determined from double-shear test with steel shear tools and from torsion tests of short tubular specimens.

<sup>b</sup>Longitudinal tensile properties determined from standard 1/2-in.-diam. tensile specimens (see reference 14, fig. 3).

<sup>c</sup>Longitudinal compressive yield strength determined from 3/4-in.-diam., 3-in.-long specimens.

<sup>d</sup>Shear yield strength determined from torsion tests of tubular specimens having D/t ratios of 10 and 15.

<sup>e</sup>Transverse tensile properties determined from A.S.T.M. standard 1/8-in.-diam. tensile specimens.

<sup>f</sup>Transverse compressive yield strength determined from 1/2-in.-diam., 1.5-in.-long specimens.

TABLE II.- DESCRIPTION OF SPECIMENS AND RESULTS OF TORSION TESTS OF 75S-T6  
TUBULAR SECTIONS MACHINED FROM 2-INCH-DIAMETER ROLLED ROUND ROD

Specimen	Dimension of reduced test section (in.)			Ratio, D/t	Ratio of length of mean radius, L/r	Maximum torque, T (ft-lb)	Corresponding average shear stress, $F_{st}$ (psi) (b)
	Outside diameter, D	Average wall thickness, t (a)	Length, L				
10	1.000	0.500	$6\frac{1}{2}$	2		1086	c49,800
11	1.249	.1245	8	9.9	14.2	1100	c53,400
12	1.153	.0765	8	15.1	14.9	580	50,000
13	1.111	.0555	8	20.0	15.2	353	43,600
1	1.527	.0760	10	20.1	13.8	940	44,800
2	1.495	.0600	10	24.9	13.9	677	41,900
3	1.473	.0490	10	30.1	14.1	542	41,700
4	1.448	.0360	10	40.2	14.2	363	38,600
5	1.433	.0293	10	48.9	14.2	274	36,200
6	1.423	.0248	10	57.4	14.3	210	33,100
7	1.410	.0175	10	80.6	14.4	91.5	20,600
8	1.527	.0747	5/8	20.4	.86	1135	c55,000
9	1.528	.0765	5/8	20.0	.86	1125	c53,400

<sup>a</sup>Maximum and minimum thicknesses measured on cut sections after tests were within  $\pm 0.002$  in. of average.

<sup>b</sup>For solid 1.000-in.-diam. specimen,  $F_{st}$  was computed on assumption of uniform stress by formula  $F_{st} = 144T/\pi D^3$ . For remaining specimens,  $F_{st}$  was computed by formula  $F_{st} = 12T/2\pi r^2 t$  where  $r$  is mean radius, in.

<sup>c</sup>Specimen fractured without buckling. All other specimens failed by buckling.

TABLE III.- DESCRIPTION OF SPECIMENS AND RESULTS OF COMPRESSION  
 TESTS OF 75S-T6 TUBULAR SECTIONS MACHINED FROM  
 2-INCH-DIAMETER ROLLED ROUND ROD

Specimen	Dimensions of reduced section (in.)		Ratio, D/t	Maximum Compressive stress (psi)	
	Outside diameter, D	Wall thickness, t (1)		First test (2)	Retest (3)
1	1.719	0.1719	10.0	99,300	-----
2	1.478	.0515	28.6	82,300	83,800
3	1.433	.0288	49.8	79,100	80,300
4	1.410	.0176	80.1	71,500	73,300
5	1.401	.0121	115.8	63,500	68,100
6	1.394	.0093	149.9	58,400	60,500

<sup>1</sup>Maximum and minimum thicknesses measured on cut specimens after test were within  $\pm 0.001$  in. of average.

<sup>2</sup>Specimens with 6-in.-long reduced section between shouldered ends as shown in fig. 4.

<sup>3</sup>Specimens having  $4\frac{1}{2}$ -in. length as shown in fig. 5, cut from undamaged portion of reduced sections after first tests.

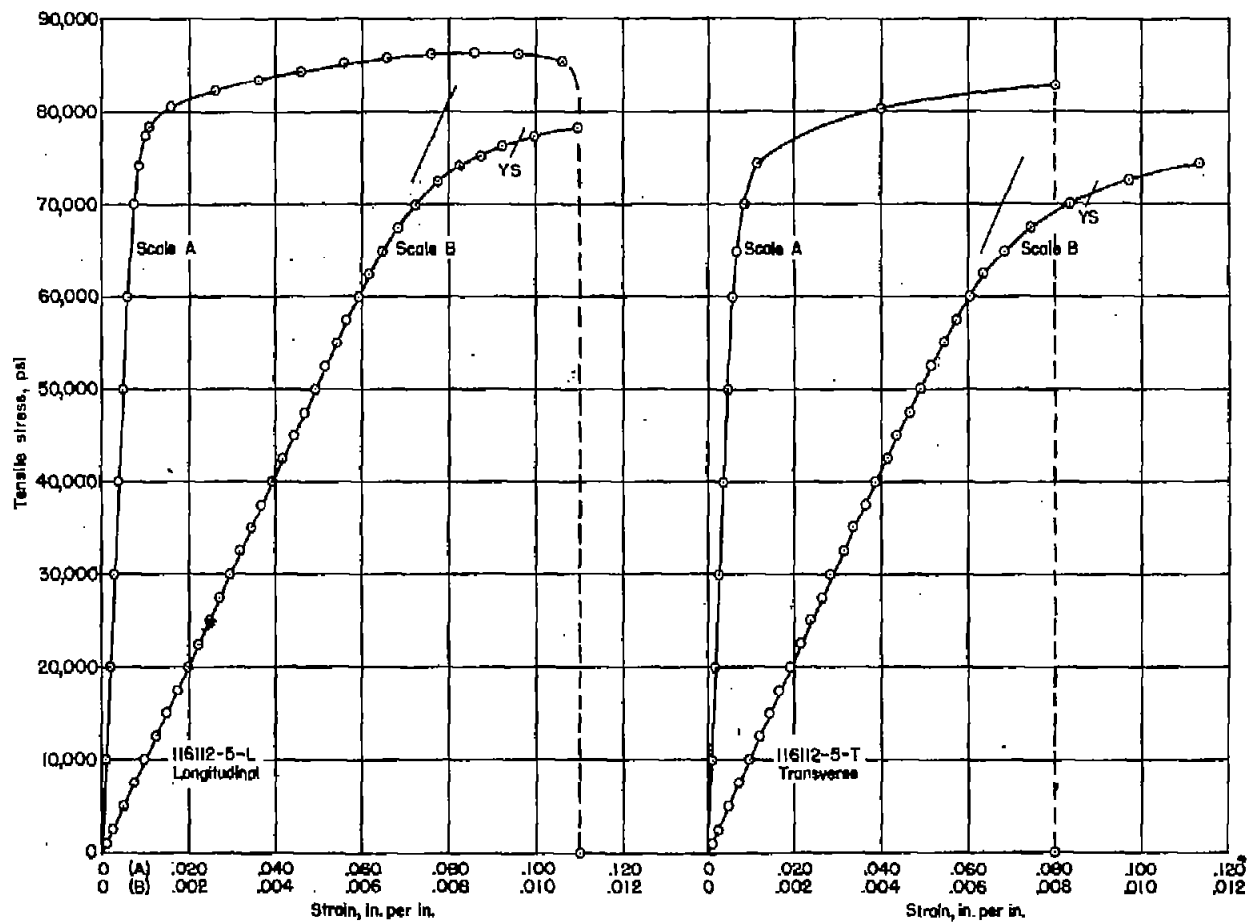
TABLE IV.- DESCRIPTION OF SPECIMENS AND RESULTS OF BENDING  
 TESTS OF 75S-T6 TUBULAR SECTIONS MACHINED FROM  
 2-INCH-DIAMETER ROLLED ROUND ROD

Specimen	Dimensions of reduced test section (in.)			Ratio, D/t	Maximum load, (lb)	Modulus of failure, $F_b$ (psi) (b)
	Outside diameter, D	Average wall thickness, t (a)	Length, L			
8	0.998	0.499	$6\frac{1}{2}$	2	c4100	157,000
11	1.250	.1250	8	10.0	c4090	133,000
12	1.154	.0770	8	15.0	2060	115,700
13	1.112	.0560	8	19.9	1280	106,700
9	1.719	.1720	10	10.0	c9600	123,700
10	1.586	.1055	10	15.0	5180	113,000
1	1.528	.0762	10	20.1	3290	107,100
2	1.497	.0609	10	24.6	2500	103,200
3	1.473	.0490	10	30.1	1840	96,400
4	1.447	.0366	10	39.5	1275	90,900
5	1.434	.0297	10	48.3	956	84,500
6	1.423	.0250	10	57.0	730	77,400
7	1.411	.0177	10	79.8	453	68,000

<sup>a</sup>Maximum and minimum thicknesses measured on cut sections after tests were within  $\pm 0.002$  in. of average.

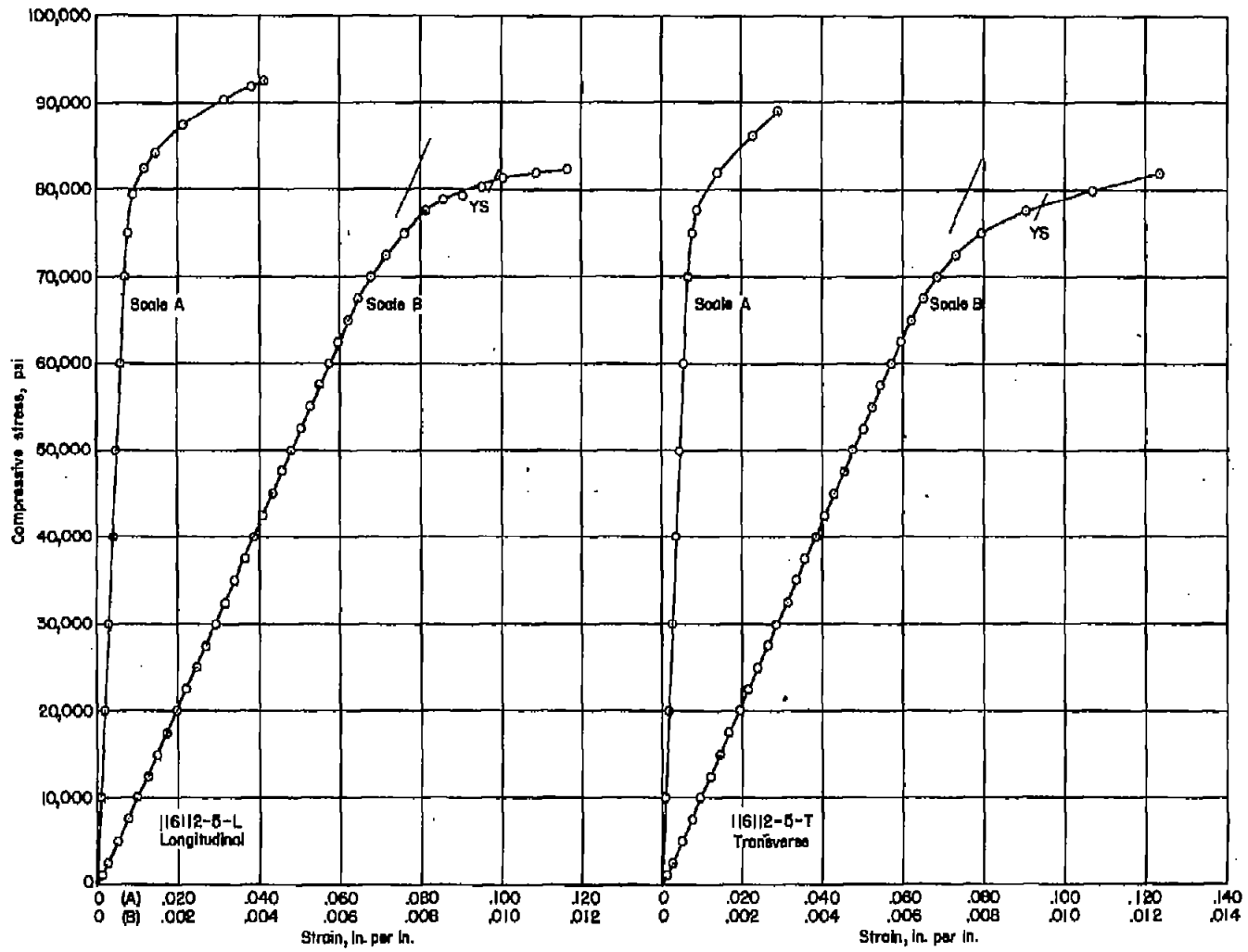
<sup>b</sup> $F_b$  was computed by formula  $F_b = Mc/I$  where M, bending moment at maximum load, in-lb;  $c = D/2$ ; and I, moment of inertia of cross section, in<sup>4</sup>.

<sup>c</sup>Load limited by deflection. All other specimens failed by buckling.



(a) Tension.

Figure 1.- Stress-strain curves of 75S-T6 aluminum-alloy rolled rod. Specimen diameter: 1/2 inch (for longitudinal), 1/8 inch (for transverse); gage length, 4D; nominal size of rod, 2 inches.



(b) Compression.

Figure 1.- Concluded.

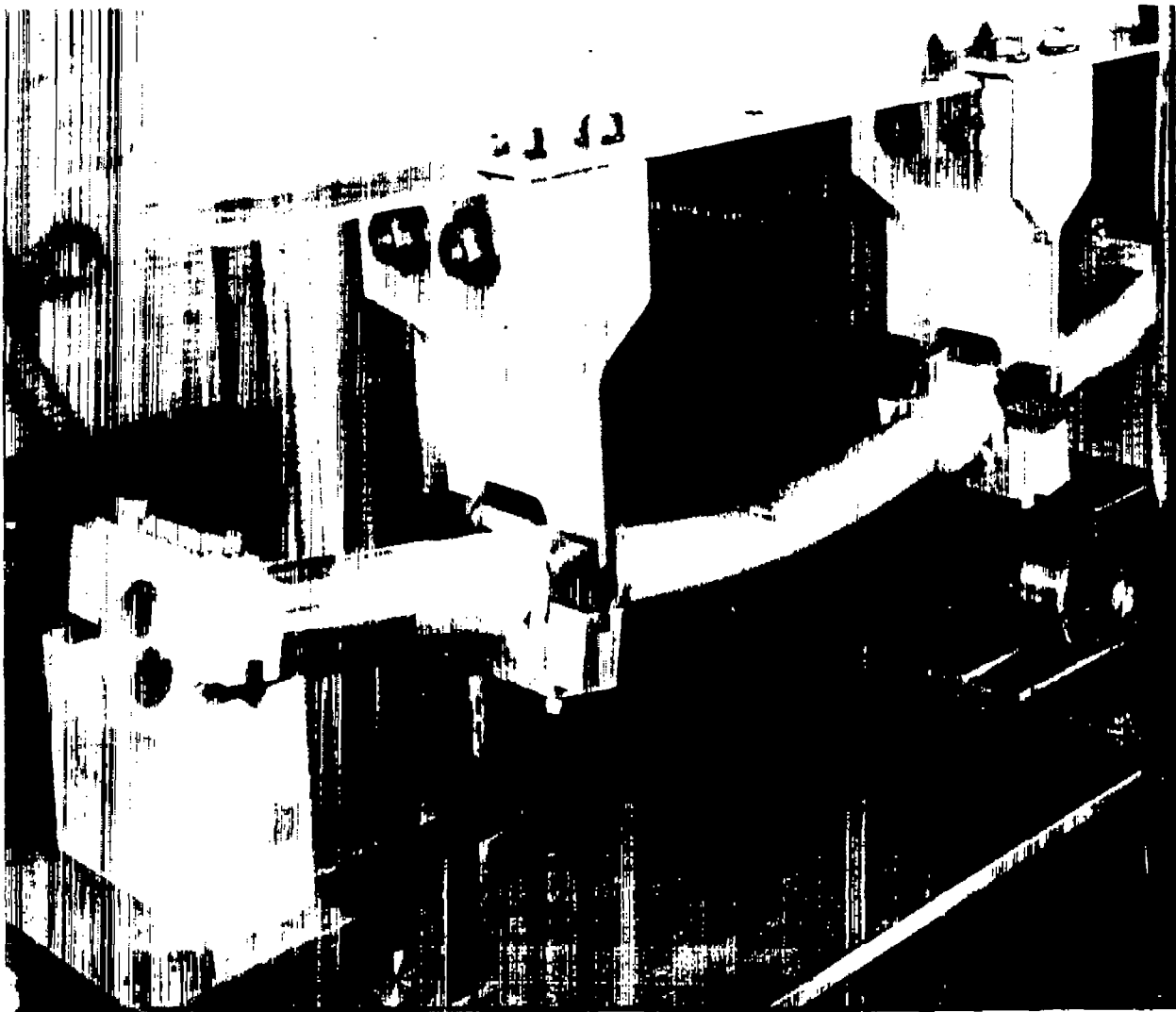
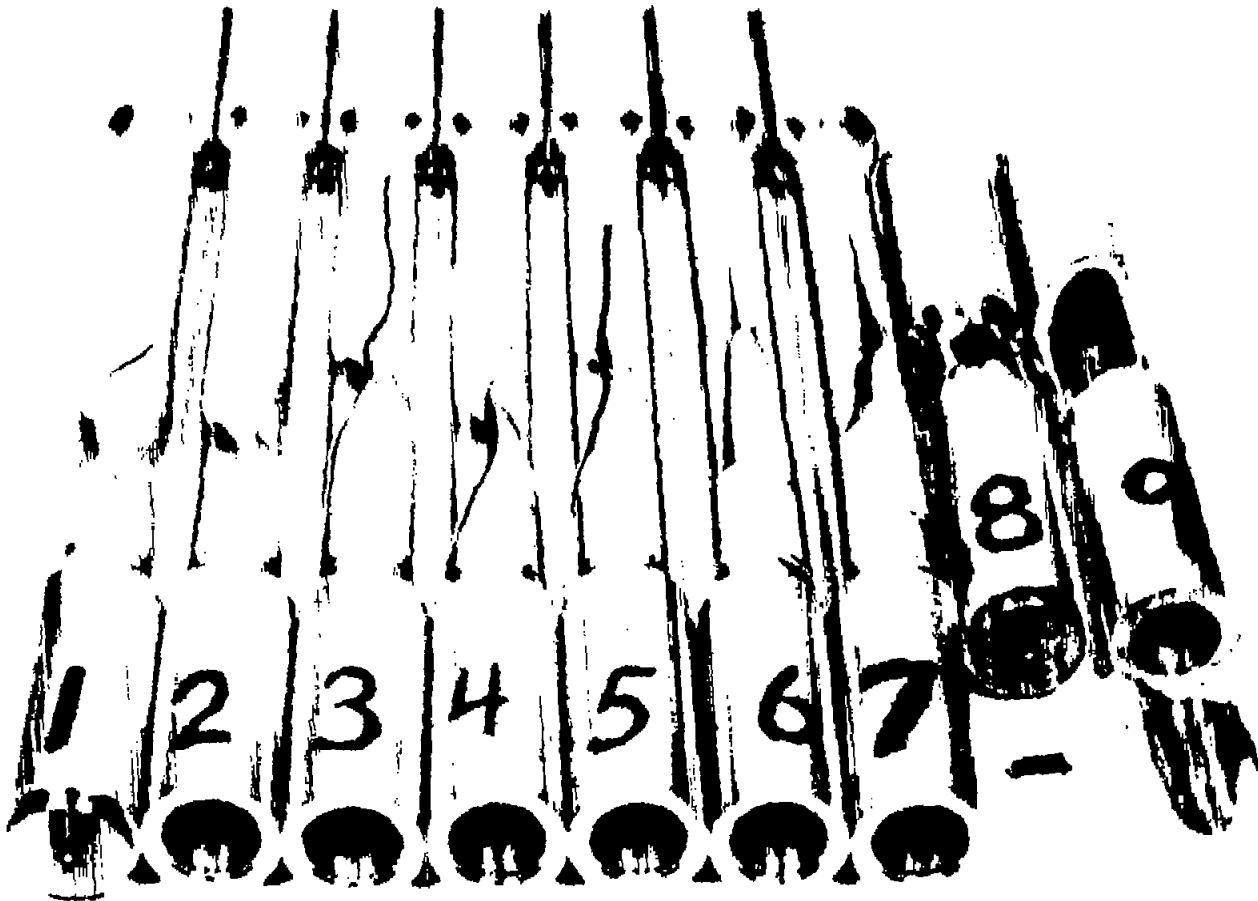


Figure 2.- Arrangement for tests under pure bending.



(a) Specimens 1 to 9.

Figure 3.- 75S-T6 specimens after failure under torsion shear.



(b) Specimens 10 to 13.

Figure 3.- Concluded.

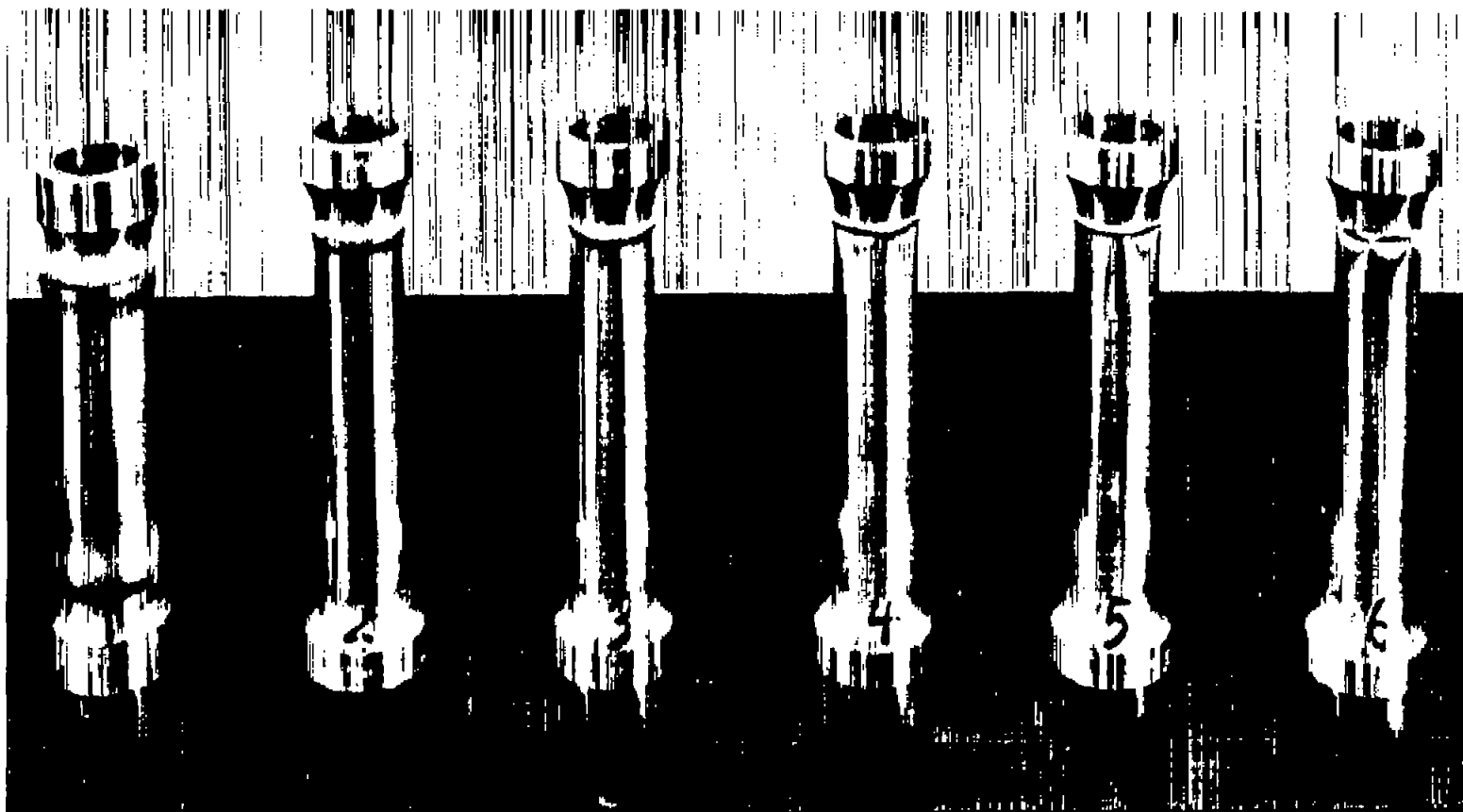


Figure 4.- 75S-T6 specimens after failure under axial compression.

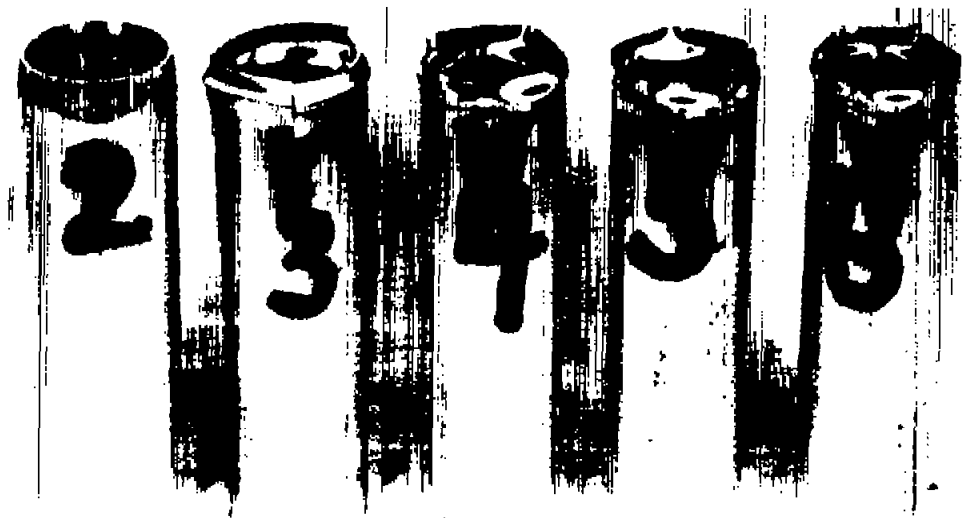
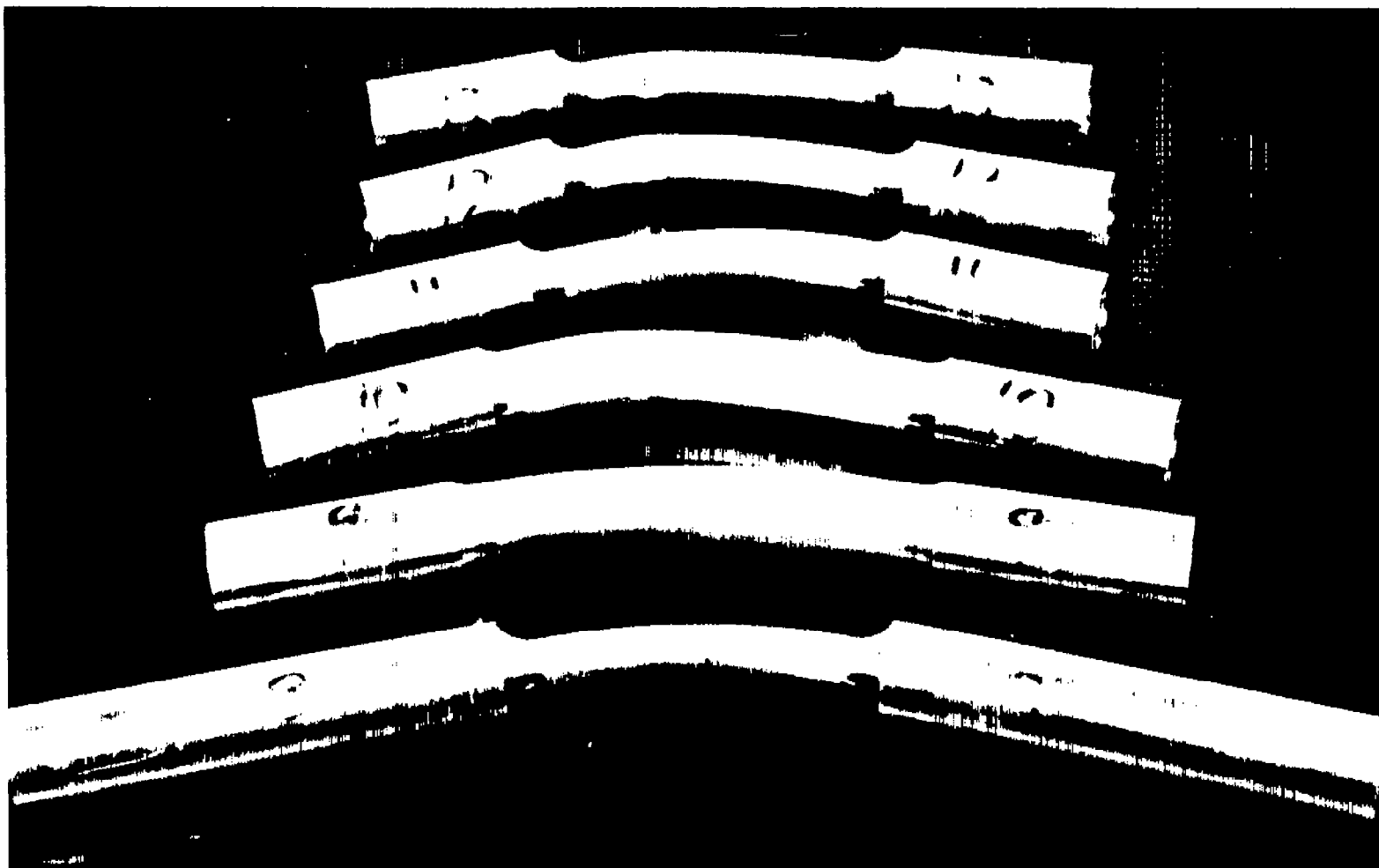


Figure 5.- 75S-T6 specimens after retest under axial compression with original reinforced ends removed.



(a) Specimens 1 to 7.

Figure 6.- Specimens after failure under pure bending.



(b) Specimens 8 to 13.

Figure 6.- Concluded.

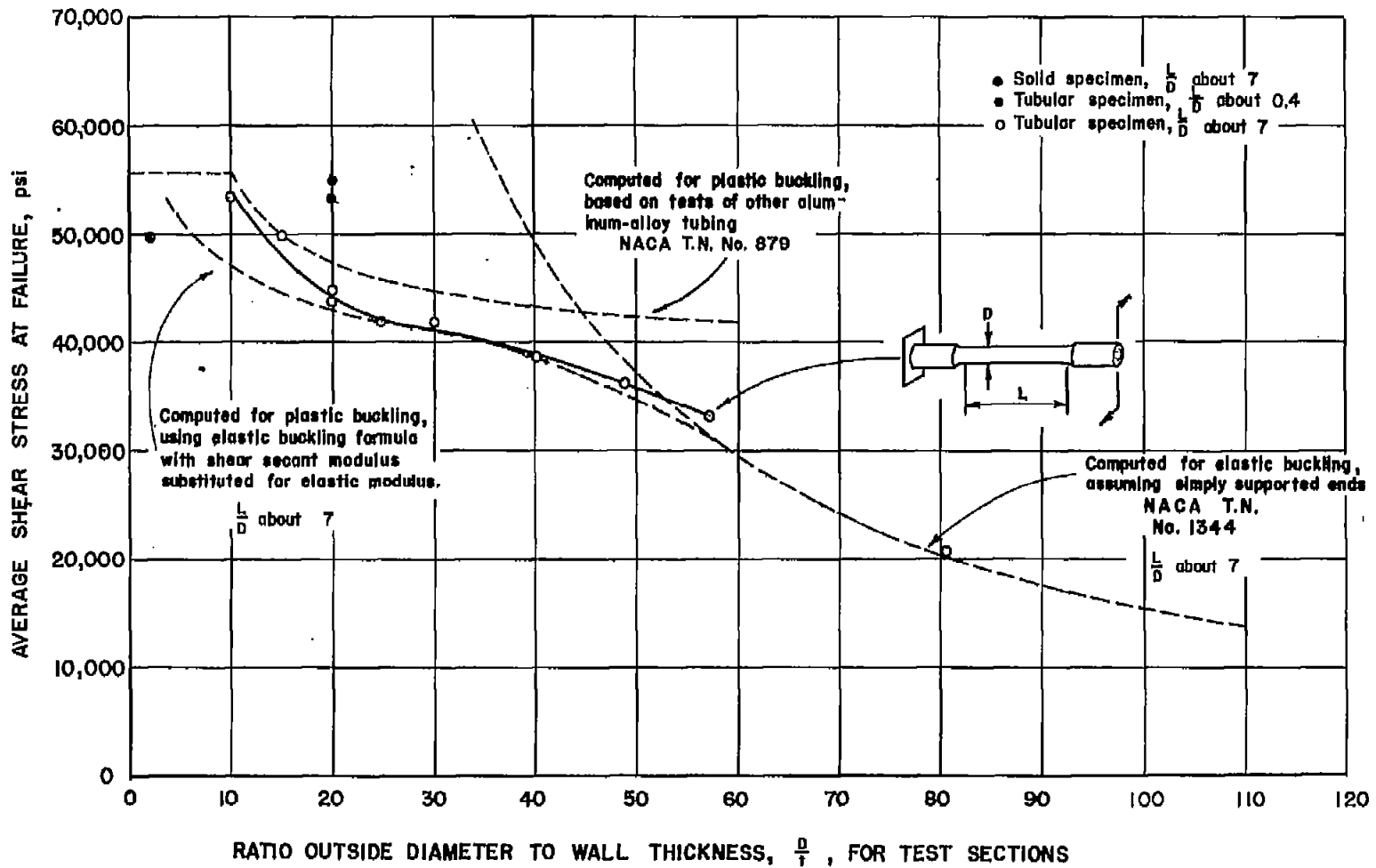


Figure 7.- Torsional strength of tubular sections machined from 758-T6 rolled rod.

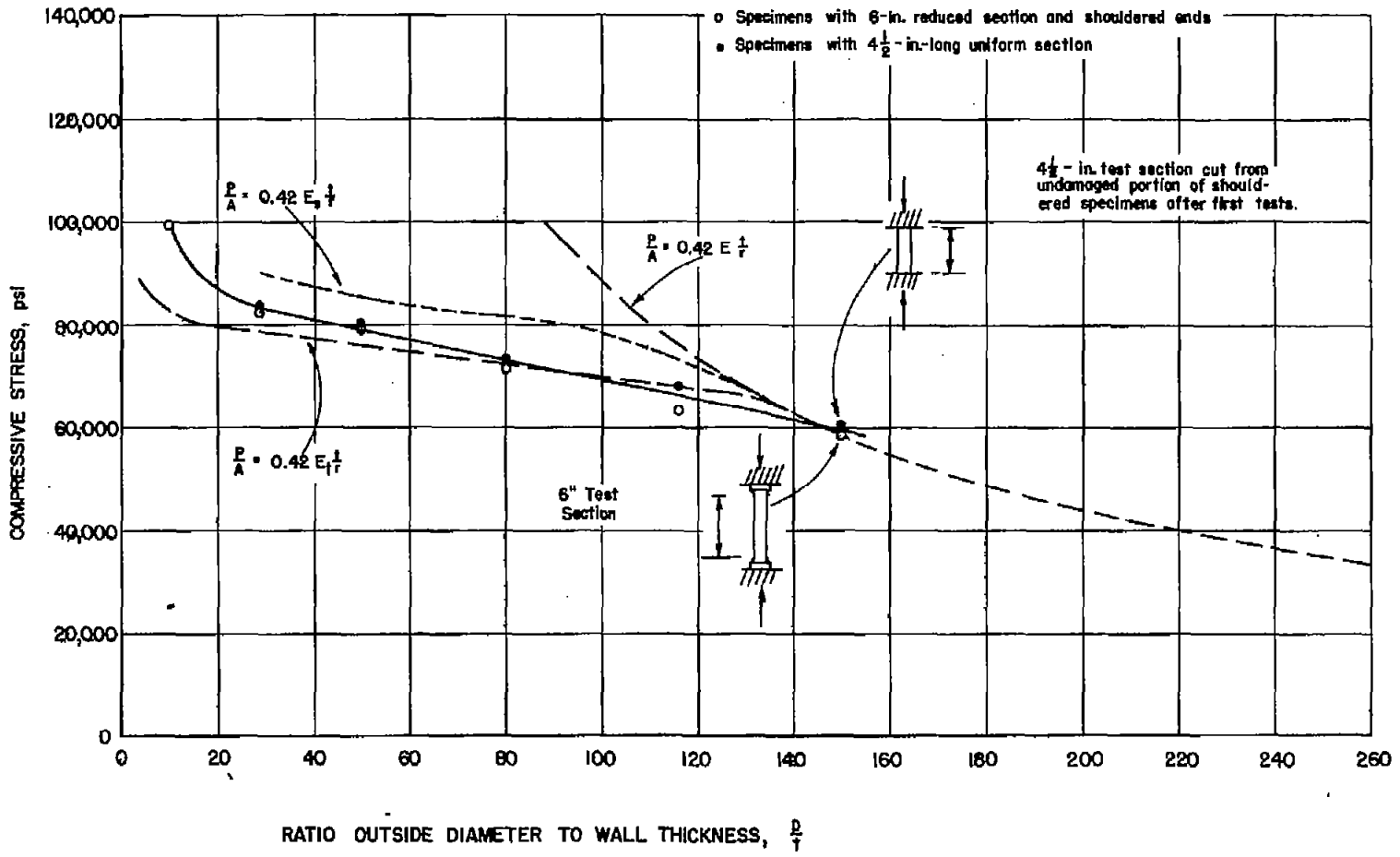


Figure 8.- Compressive strength of tubular sections machined from 75S-T6 rolled rod.

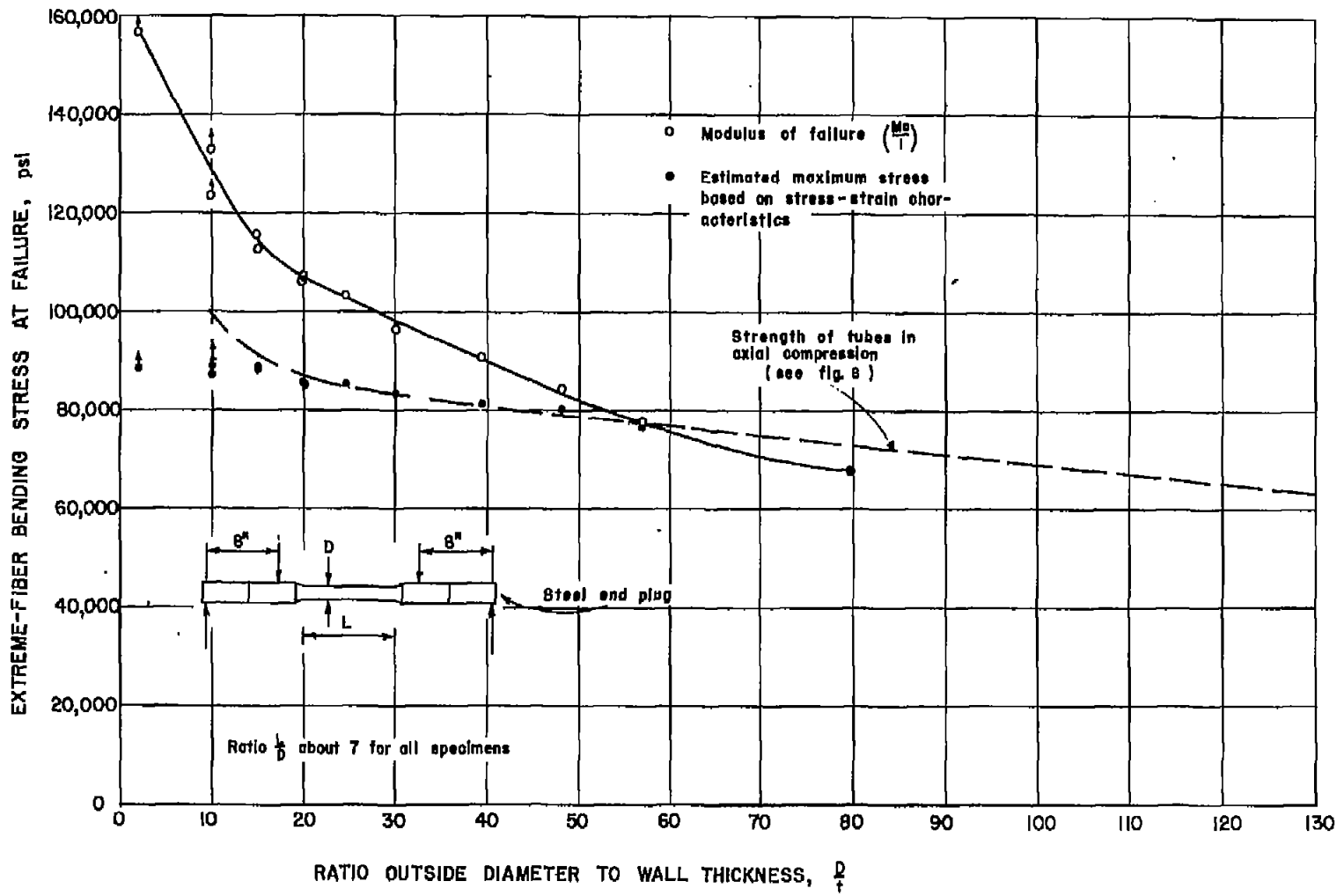
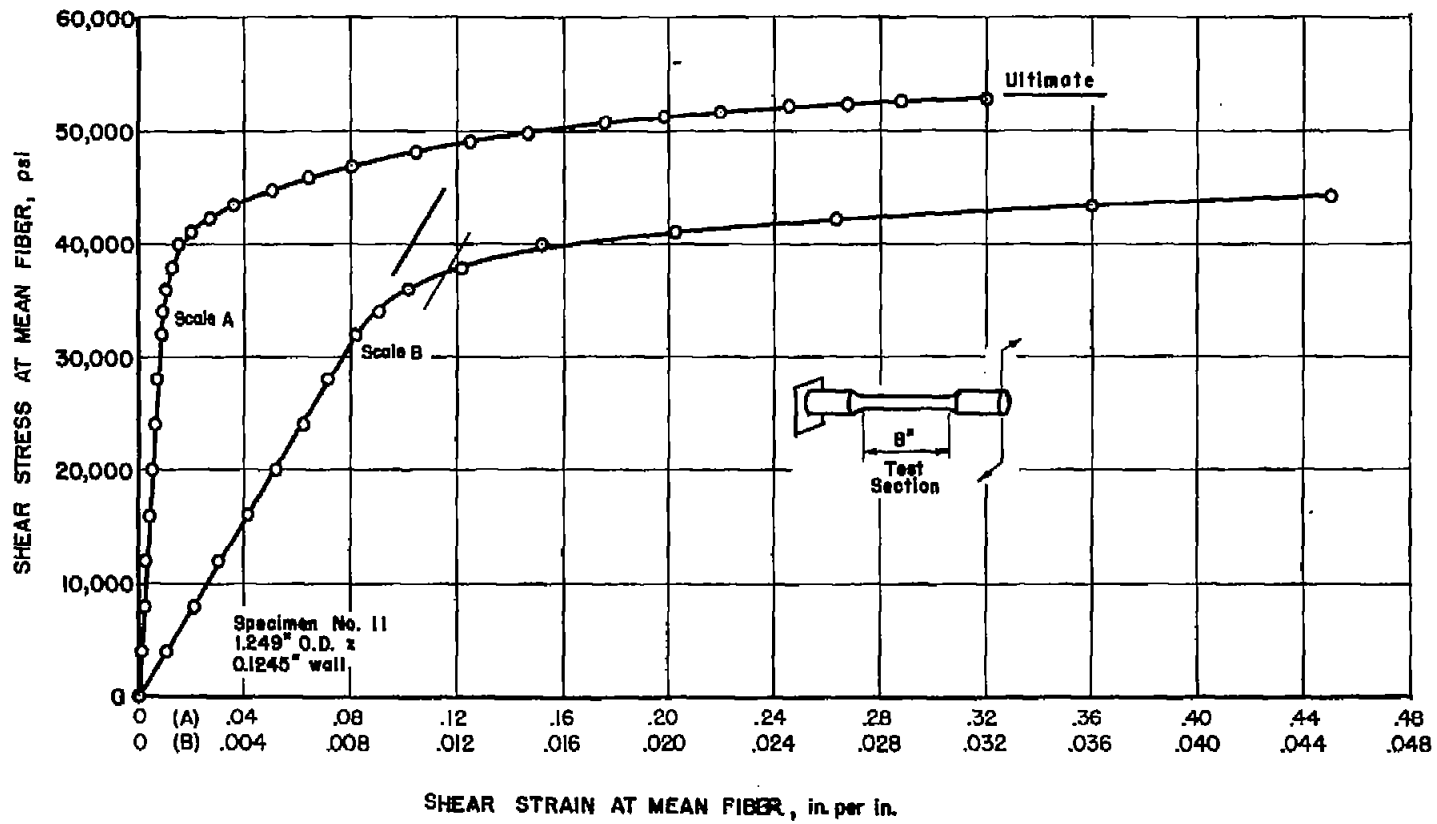
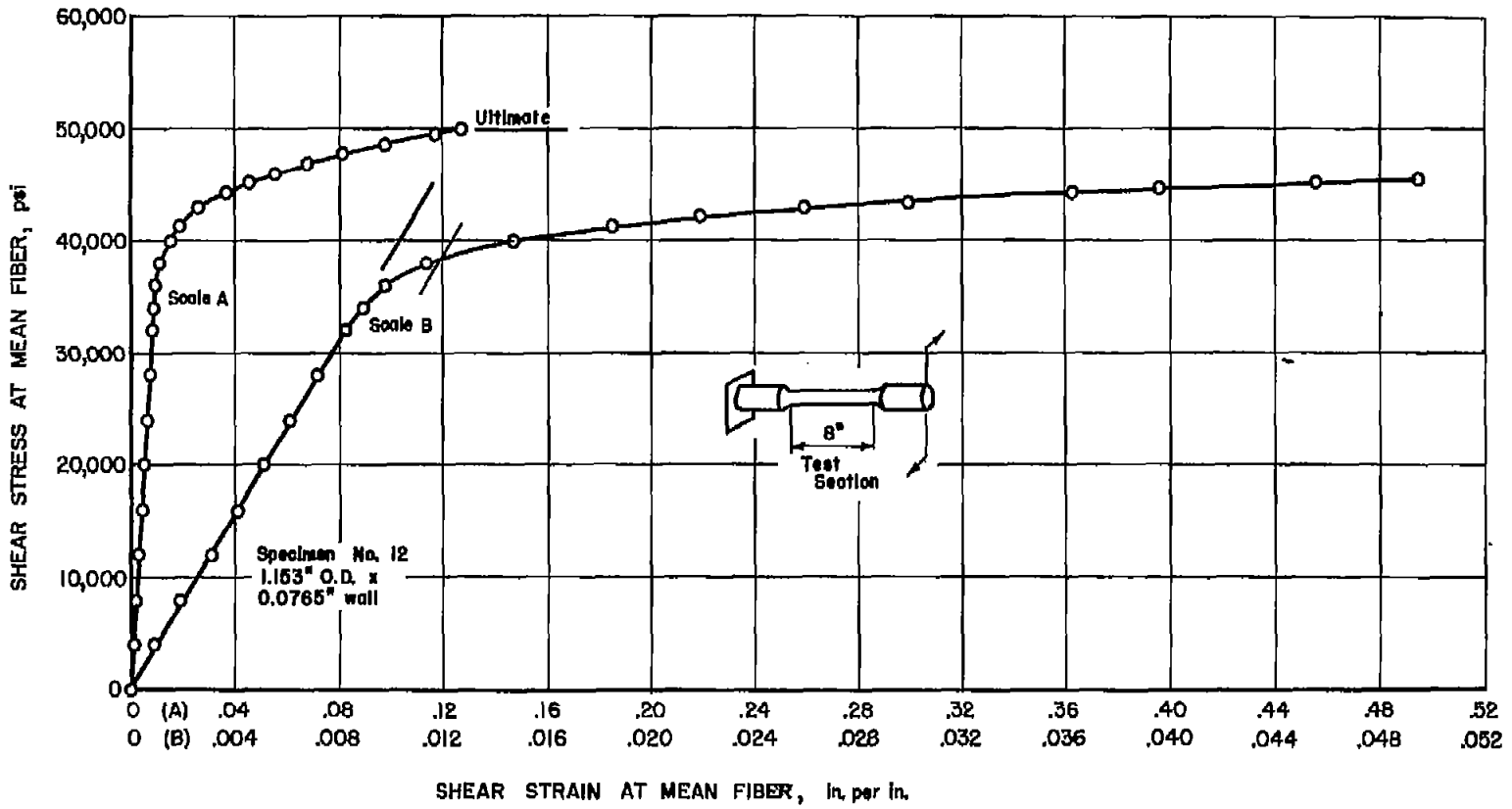


Figure 9.- Bending strength of tubular sections machined from 75S-T6 rolled rod.



(a) Specimen 11.

Figure 10.- Shear stress-strain curves for torsion specimens 11 and 12 machined from 75S-T6 rolled rod.



(b) Specimen 12.

Figure 10.- Concluded.

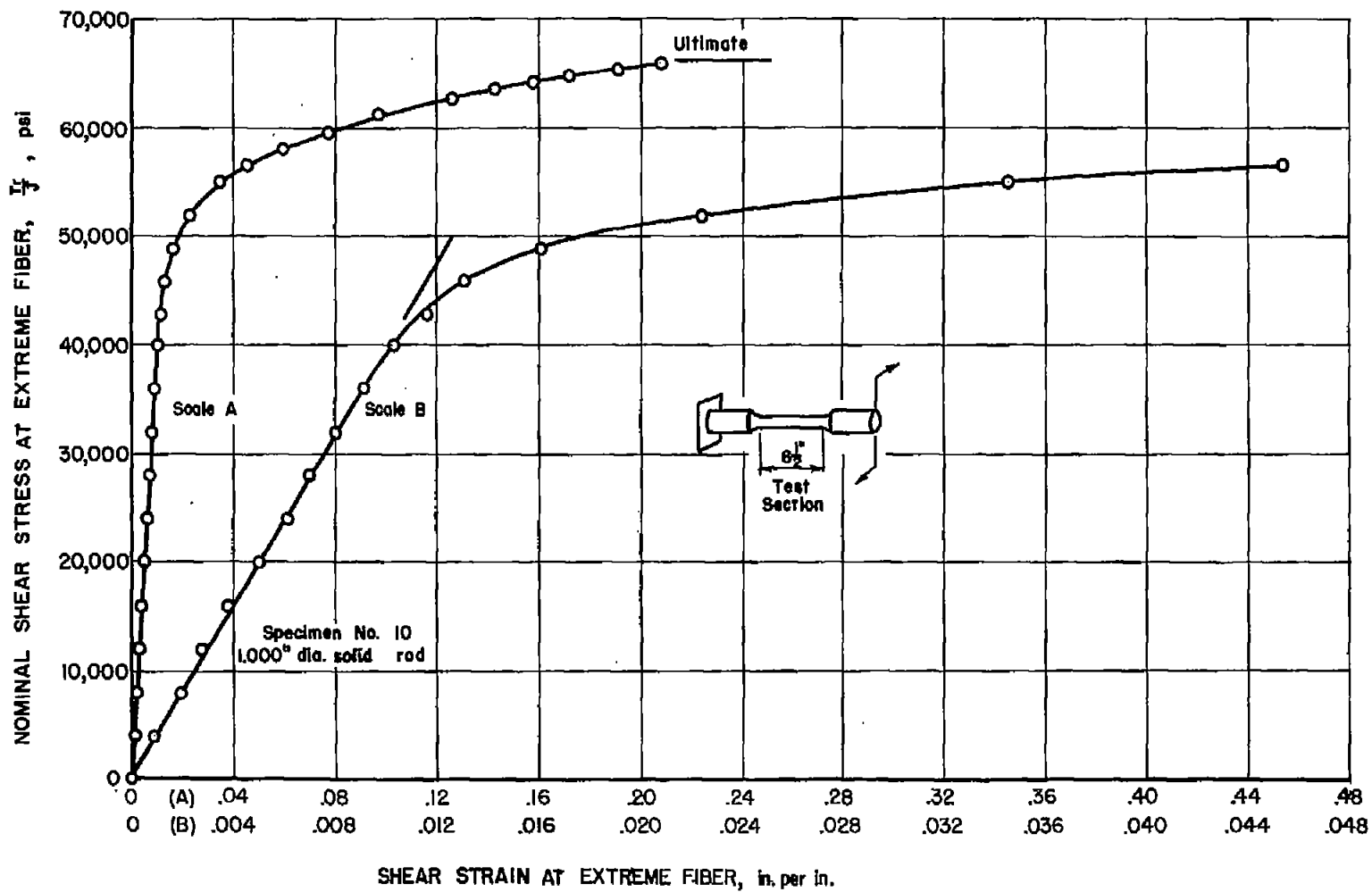
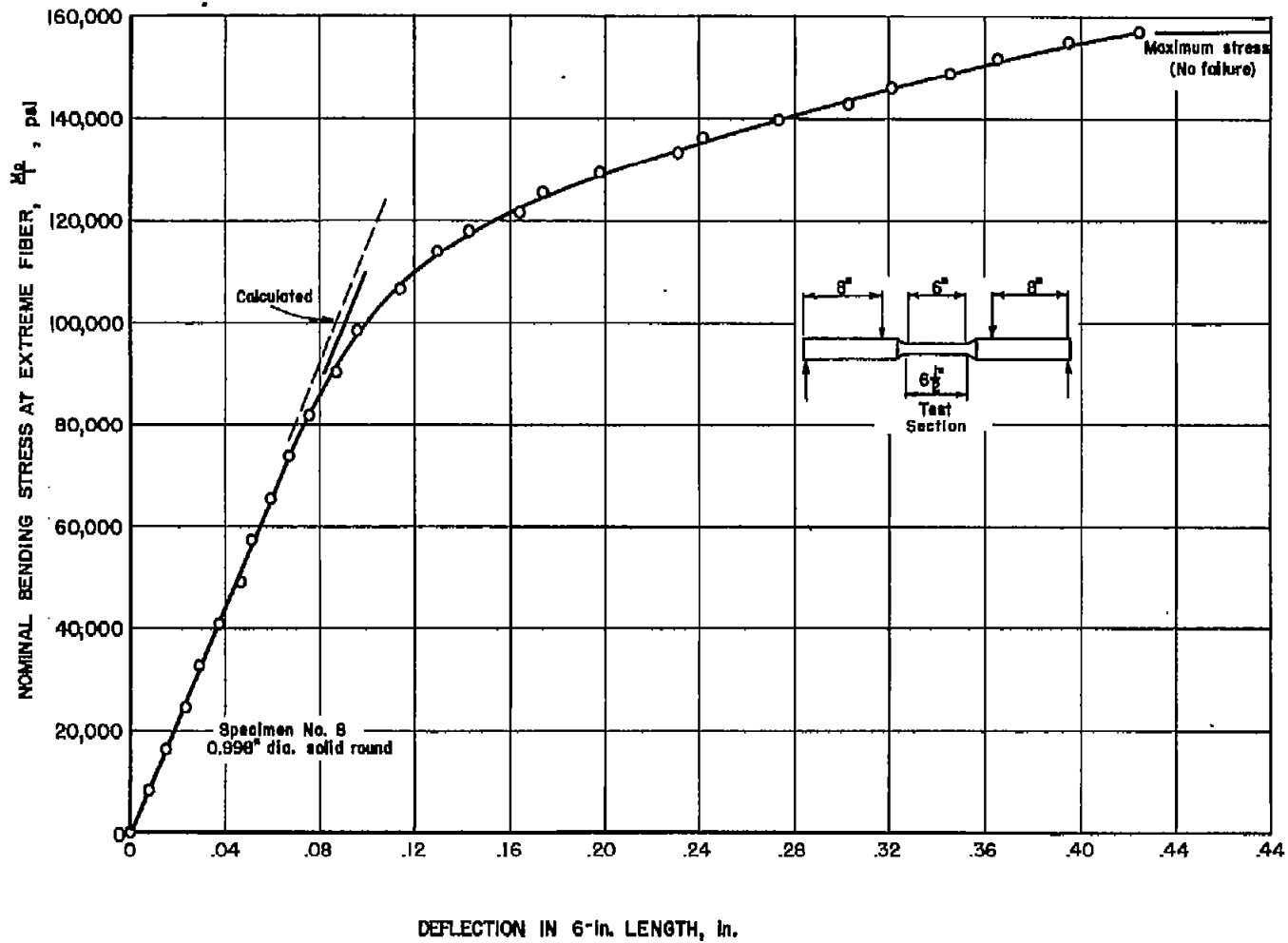
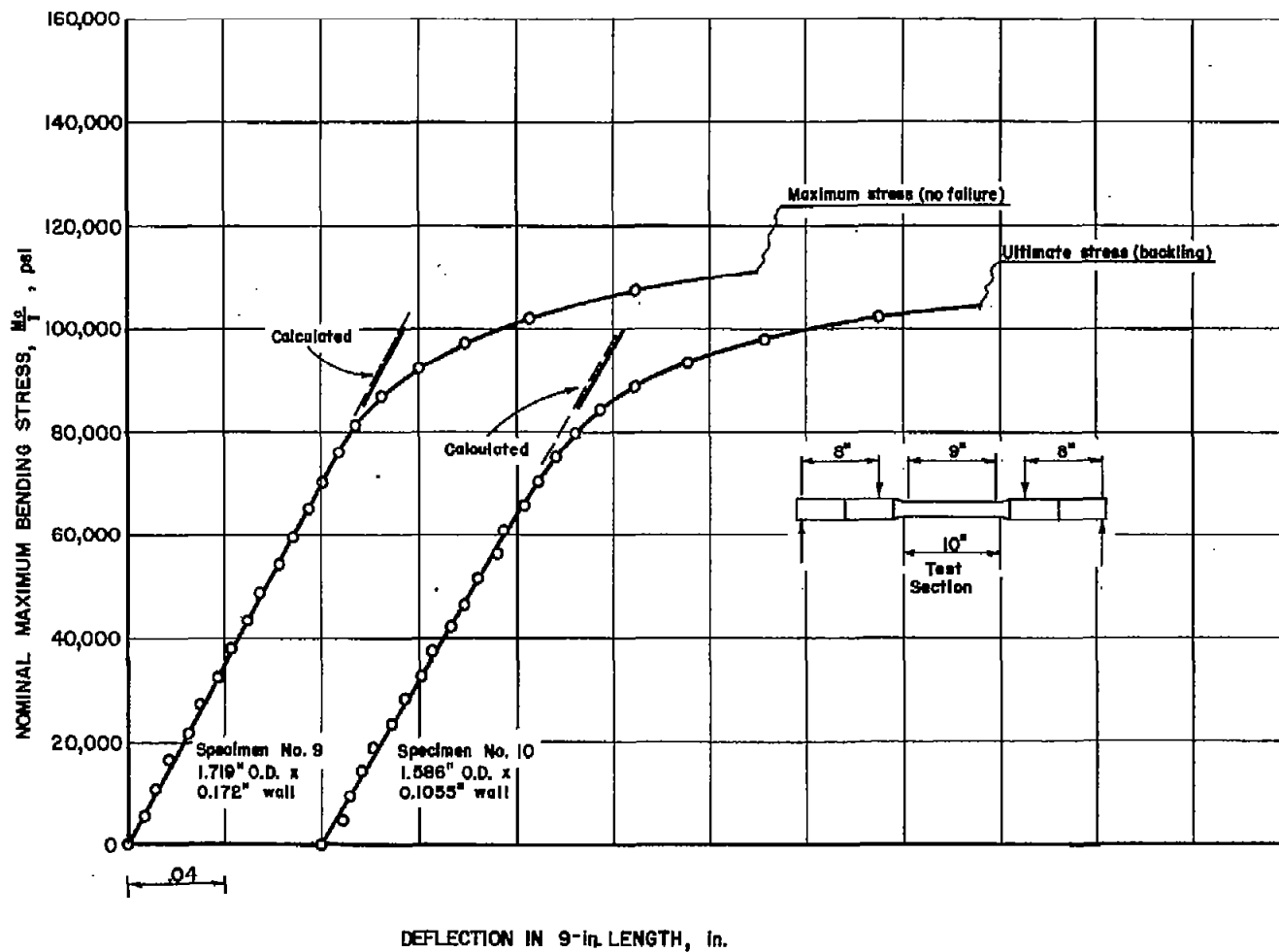


Figure 11.- Nominal shear stress-strain curve for torsion specimen 10 machined from 75S-T6 rolled rod.



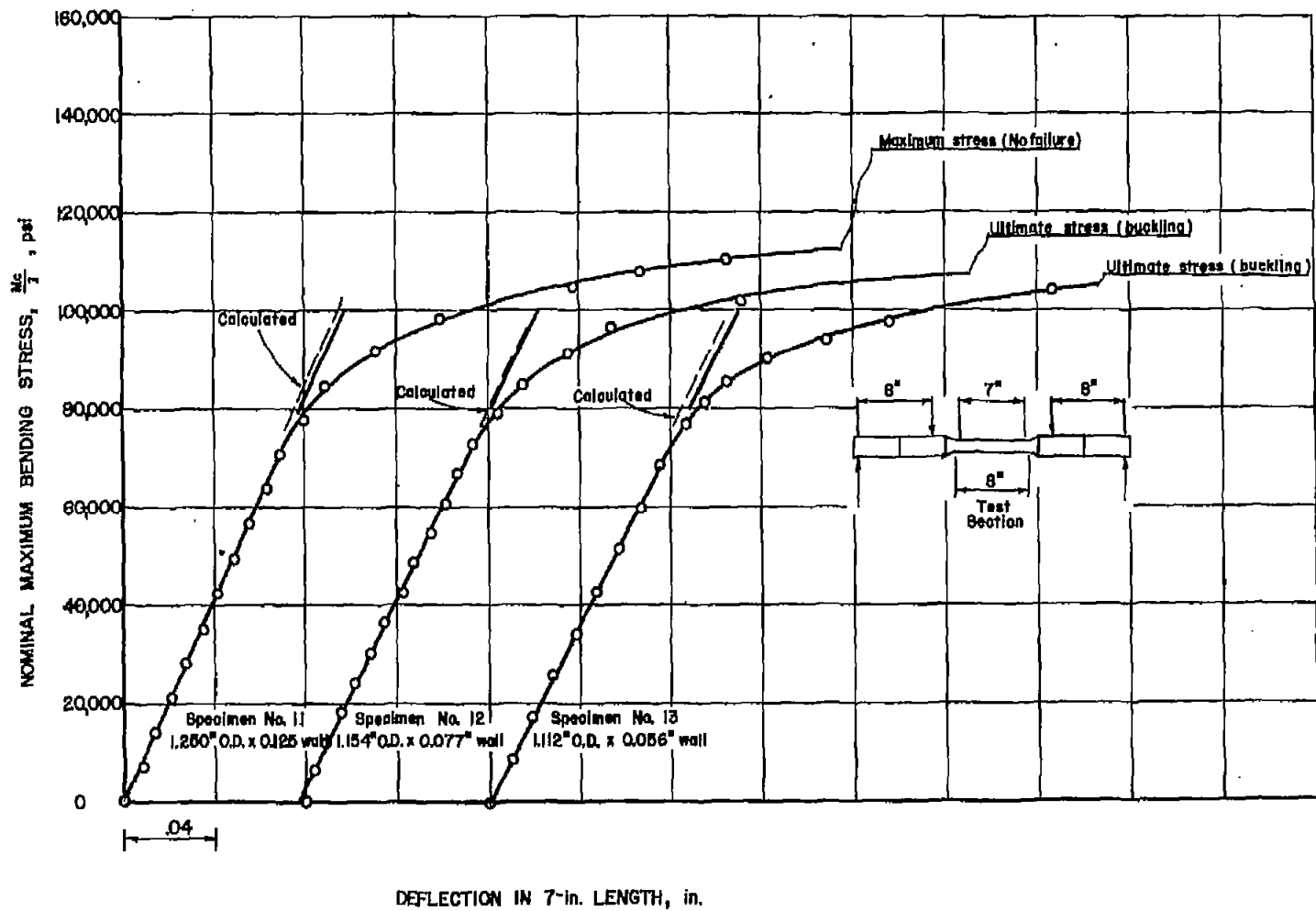
(a) Specimen 8.

Figure 12.- Stress-deflection curves for bending specimens 8 to 13 machined from 75S-T6 rolled rod.



(b) Specimens 9 and 10.

Figure 12.- Continued.



(c) Specimens 11, 12, and 13.

Figure 12.- Concluded.